JOURNAL OF SYNCHROTRON RADIATION

ISSN 1600-5775

Received 20 April 2018
Accepted 13 July 2018

Edited by G. Grübel, HASYLAB at DESY, Germany

Keywords: THz; on chip; spectrometer; bunch compression; X-ray free-electron laser.

On-chip THz spectrometer for bunch compression fingerprinting at fourth-generation light sources

M. Laabs,[a] N. Neumann,[a]* B. Green,[b] N. Awari,[b] J. Deinert,[b] S. Kovalev,[b] D. Plettemeier[a] and M. Gensch[b]*

[a]Communications Lab, TU Dresden, 01062 Dresden, Germany, and [b]Helmholtz-Zentrum Dresden-Rossendorf, Bautzner Landstraße 400, 01328 Dresden, Germany. *Correspondence e-mail: niels.neumann@tu-dresden.de, m.gensch@hzdr.de

The layout of an integrated millimetre-scale on-chip THz spectrometer is presented and its peformance demonstrated. The device is based on eight Schottky-diode detectors which are combined with narrowband THz antennas, thereby enabling the simultaneous detection of eight frequencies in the THz range on one chip. The size of the active detector area matches the focal spot size of superradiant THz radiation utilized in bunch compression monitors of modern linear electron accelerators. The 3 dB bandwidth of the on-chip Schottky-diode detectors is less than 10% of the center frequency and allows pulse-resolved detection at up to 5 GHz repetition rates. The performance of a first prototype device is demonstrated at a repetition rate of 100 kHz at the quasi-cw SRF linear accelerator ELBE operated with electron bunch charges between a few pC and 100 pC.

1. Introduction

Robust techniques and devices for measuring the spectrum of THz radiation are of high technological interest (see, for example, Dhillon *et al.*, 2017). While the matured development of laser-based techniques such as electro-optic sampling allows measurement of THz spectra with large dynamic range and excellent spectral resolution, there still exists a high demand for easy-to-implement compact devices for application in surveillance or monitoring in complex environments, for example (Dhillon *et al.*, 2017; Ho *et al.*, 2008; Sokolnikov, 2013). One such application is the monitoring of the superradiant THz emission from relativistic electron bunches in modern electron linear accelerators (linacs) (Schmidt *et al.*, 2018). The acceleration of ultra-short electron bunches in linacs has in the past 20 years emerged as key technology to provide coherent photon pulses with unique properties in a wide spectral range from the THz to the X-ray regime. In particular, X-ray free-electron lasers (XFELs) are based on kilometre-long accelerators and are required to function reliably in 24/7 user operation (Waldrup, 2014; Ball, 2017). Constant online surveillance along the accelerator and appropriately fast feedback loops are required to keep the most important electron bunch properties, *i.e.* arrival time, charge, position and form, stable in order to minimize the instabilities in the generated photon pulses. The current state-of-the-art approach employs two fundamental detector types in order to determine changes of these properties with high precision. The arrival time of the electron bunches with respect to a synchronized reference laser is measured at various locations along the linac by means of compact so-called bunch arrival time monitors (BAMs) (Löhl *et al.*, 2010) based on electro-optic detection of the Coulomb field of the

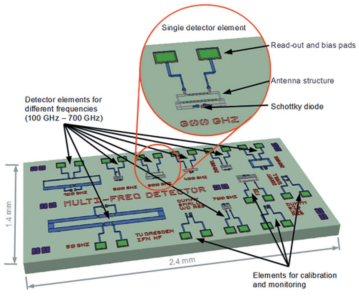

bunches. The bunch charge and position are detected sensitively by compact so-called beam position monitors (BPMs) based on electric detection of the passing Coulomb field (Keil *et al.*, 2010, 2014), while changes of the bunch form are typically monitored by detecting the intensity of the emitted superradiant THz radiation in the far-field by single-element broadband detectors in compact so-called bunch compression monitors (BCMs) (Dunning *et al.*, 2007).

The latter type of monitor thereby provides one value for a clearly multi-dimensional property such as the bunch form which can be, for example, affected by bunch duration and shape. Hence, different types of spectrometers have been tested and installed at typically one exclusive position along the linacs. While for mathematical reasons the emitted THz spectrum unfortunately does not allow unequivocal determination of the bunch form or bunch duration (Schmidt *et al.*, 2018), it has been successfully shown that it can indeed act as a very helpful characteristic fingerprint for a particular optimal bunch compression setting (Nodvick & Saxon, 1954; Lai & Sievers, 1997; Murokh *et al.*, 1998; Watanabe *et al.*, 2002; Casalbuoni *et al.*, 2009; Wesch *et al.*, 2011; Maxwell *et al.*, 2013). The primary requirement for such a monitor is hence not to provide an accurate THz spectrum but to provide a precise measurement of the relative changes of the THz intensities in different spectral regions over time. Here we present a THz spectrometer that makes a compromise between robustness, compactness, sensitivity and achievable frequency resolution and provides fingerprint THz spectra at high dynamic range and with a detector bandwidth that in principle allows pulse-resolved detection up to 5 GHz repetition rates. It thereby is not only applicable at linacs for fourth-generation light sources such as XFELs (Ackermann *et al.*, 2007; Emma *et al.*, 2010; Altarelli, 2011; Galayda, 2014; Kang *et al.*, 2017; Ishikawa *et al.*, 2012) but can also be employed at, for example, future energy-recovery-linac-based light sources (Cornell, 2013; Abo-Bakr *et al.*, 2012).

2. Results

The detection of THz signals can be carried out using many mechanisms and materials (Brown, 2015), *e.g.* thermal detection, high-electron-mobility transistor (HEMT) or metal oxide semiconductor (MOS) based detection and E-field rectification. Semiconductor-based THz detectors have the advantage of robust operation at room temperature and potentially low cost. Additionally, semiconductor devices offer the detection of high repetition rates up to GHz (*e.g.* in contrast to pyroelectric detectors). The transit frequency of semiconductor transistors is usually lower than the cut-off frequency of diodes. The semiconductor devices with the highest frequencies usable for THz detection are manufactured in III/V semiconductor processes (Mehdi *et al.*, 2017). Possible applications cover metrology, space and imaging.

The technology chosen for the spectrometer chip is based on integrated gallium arsenide (GaAs) Schottky diodes. This approach has been previously developed commercially for microwave monolithically integrated circuits (MMICs) such as mixer and power detectors. With minor layout modifications, these diodes ensure robust operation at room temperature, and compactness of the complete device matching well with the limited space in modern accelerator tunnels. The manufacturing process is evaluated for MMICs in space (Kayali *et al.*, 1996; ESCC, 2014) and is therefore radiation tolerant. Furthermore, reasonable low-cost mass production is possible, which is important for the application as envisioned 'field' THz monitors at multiple positions along often kilometre-long linacs. The fundamental concept is shown in Fig. 1. Schottky diodes connected to narrowband on-chip antennas (Schiselski *et al.*, 2016) provide frequency selectivity. Each detector consists of a Schottky diode and a narrowband capacitively coupled closed-loop antenna with gamma match. This way, different narrow frequency bands are sliced out of a broad THz spectrum and the power within these bands can be detected yielding a spectral resolution. The realized on-chip spectrometer holds eight receiving antenna structures, each

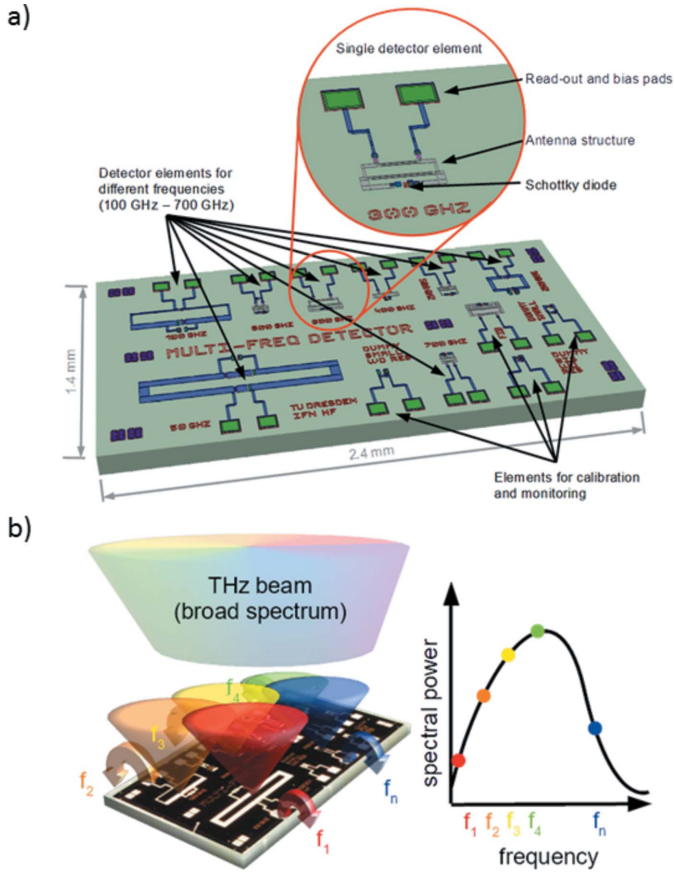

Figure 1
(*a*) Fundamental layout of the compact integrated THz spectrometer based on Schottky diodes coupled to frequency-selective antenna structures. The chip is 2.4 mm × 1.4 mm wide. Each detector element can be read out and biased individually. The 50 GHz detector element is for monitoring possible strong interfering signals at comparably low frequencies. The remaining seven elements from 0.1 to 0.7 THz are used to sample the spectral behavior. (*b*) Application as detector for THz fingerprint spectra. When irradiated with a broadband THz spectrum such as a superradiant pulse from an ultra-short relativistic electron bunch, different frequency components can be detected in parallel and relative changes can be monitored with high precision.

connected to a Schottky diode detector. The frequency bands range from 0.1 THz to 0.7 THz. The 50 GHz element detects interfering signals at comparably low frequencies and high powers. The spectral width of the frequency bands is expected to be between 4 and 20% of the center frequency, *i.e.* a few 10 GHz in the frequency bands of operation (see Table 1).

Table 1
Simulated bandwidth (BW) of the antenna structures.

Antenna	50 GHz	100 GHz	200 GHz	300 GHz	400 GHz	500 GHz	600 GHz	700 GHz
BW (GHz)	6	13	42	15	17	19	26	28
BW (%)	11	13	21	5	4	4	5	4

Antenna structures for frequencies above 200 GHz require a thinner GaAs substrate of 20 µm. Therefore, a glass-mask-based grinding and polishing process was developed for chip thinning. The respective frequency components in a THz beam irradiating this area can thereby be detected with a frequency resolution given by the central frequency and the bandwidth of the antenna–detector structures (see Fig. 1*b*). The spectrometer chip has been tested at the SRF accelerator-based TELBE light source (Schiselski *et al.*, 2016), which currently provides THz pulses in a frequency range between 0.1 and 1.2 THz at a repetition rate of beyond 100 kHz. THz pulses from the TELBE diffraction radiator source were focused onto the THz chip spectrometer by a short-focal-length off-axis parabola (see Fig. 2). Due to the characteristics of the diffraction radiator source (Green *et al.*, 2016), the beam profile consists of two lobes with the main intensity irradiating an area of roughly 4 mm in diameter. The THz beam can be dimmed by means of a combination of wire-grid polarizers. A polarizing beamsplitter was used to guide a part of the beam onto a reference detector. Various options for primarily laser-based spectroscopies can be employed to characterize the THz properties in the time and frequency domain. In Fig. 3(*a*) the time-domain measurement of the THz pulses used to benchmark the detector chip is shown. The THz pulses have a duration of below 2 ps. For this test, the readout electronics were optimized to the nominal highest repetition rate of the ELBE accelerator of 13 MHz. This improves noise performance and relaxes data acquisition requirements at the expense of video bandwidth. The detector response time is below 77 ns and hence matched the requirements as can be seen in Fig. 3(*b*) where the detector signal from a single THz pulse is shown.

The dynamic range of the THz spectrometer was then subsequently tested by measuring THz spectra for different bunch charges (see Fig. 4*a*). The sensitivity is evidently sufficient to detect a meaningful THz spectrum and in particular also relative changes of the different spectral components sensitively down to the lowest charge of 2.5 pC which corre-

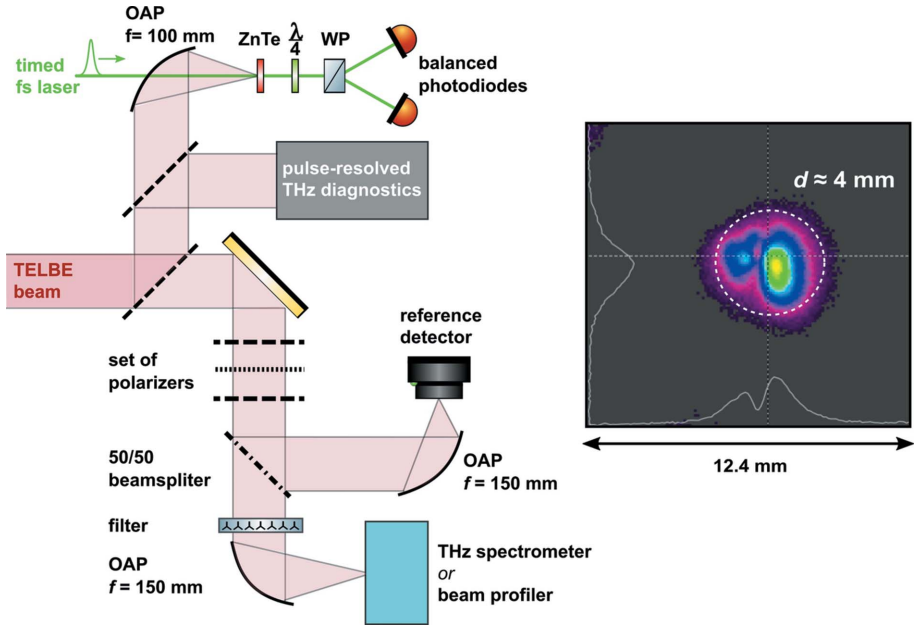

Figure 2
(Left) Experimental setup for the benchmarking of the THz spectrometer chip. The TELBE beam can be dimmed by means of a set of polarizing filters based on wire grids. Part of the beam can be taken to a calibrated reference detector. The spectral content of the beam can be filtered by THz bandpass filters. The beam can also be taken to a novel pulse-resolved THz diagnostic setup based on single-shot electro-optic sampling (Kovalev *et al.*, 2017) and to a time-domain spectroscopy set-up (top). (Right) Image of a typical beam profile after focusing by a 150 mm focal length off-axis parabola. The dimensions are in the few millimetre range and hence of the order of the THz spectrometer chip.

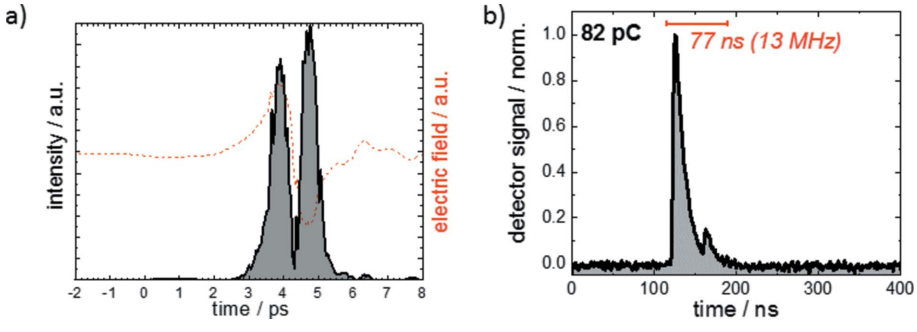

Figure 3
Bandwidth of the detector chip. (*a*) THz pulse form and duration from electro-optic sampling. (*b*) Single-shot detector response of the 0.4 THz element determined for a 82 pC bunch charge with a 4 GHz oscilloscope.

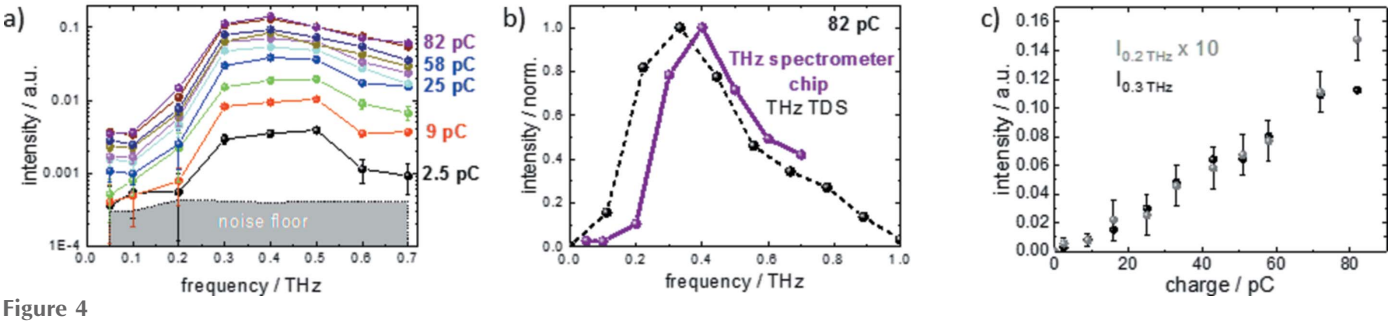

Figure 4

Benchmarking of the spectrometer chip. (*a*) THz spectra for different charges between 2.5 and 82 pC. Error bars determined from the noise band with absent signal are also given. The spectrometer chip is able to detect single THz pulses down to 2.5 pC with sufficient dynamic range. (*b*) Comparison of the THz spectra for a bunch charge of 82 pC as determined by the THz spectrometer chip (purple solid) and by THz TDS (dashed). (*c*) Charge dependence of the intensity as detected with the 0.2 and 0.3 THz element.

sponds to a top-down estimate of the pulse energy in the few 100 pJ regime. The noise floor of the current chip is given by the RMS noise floor of the oscilloscope (mainly digitizer noise) utilized for the read-out and can be further optimized. Comparing the determined THz spectrum by the chip with that of a subsequent THz time-domain measurement shown in Fig. 4(*b*) reveals a surprisingly good qualitative agreement, despite the fact that no care was taken to calibrate the detector response or compensate for detector nonlinearities and that the chip was positioned in the beam by optimizing the intensity of the 0.2 THz and 0.3 THz antenna for the 100 µm- and 20 µm-thick chip.

3. Conclusion

A compact robust THz spectrometer chip has been developed and tested at the superradiant THz facility TELBE. The detector bandwidth of the presented spectrometer chip allows single-pulse detection up to 5 GHz repetition rate. The current electronic readout circuitry of the chip is optimized for repetition rates of 13 MHz and below. It thereby matches the requirements for bunch compression fingerprinting at the ELBE facility (Gabriel *et al.*, 2000) (13 MHz), the European XFEL (Altarelli, 2011) (4.5 MHz) and the LCLSII XFEL (Galayda, 2014) (1 MHz). Note that the GeV-scale linear accelerators at the European XFEL and the LCLSII XFEL generate considerably larger THz pulse energies than the few 10 MeV ELBE linac. The ability of the THz spectrometer chip to measure THz fingerprint spectra for charges down to the few pC regime at TELBE hence ensures suitability for all types of operation in these facilities including low charge operation as recently developed for single-mode lasing (Marchetti *et al.*, 2014). Efforts are underway to utilize plasma wave effects to realize detectors with higher sensitivity. Furthermore, broadband as well as frequency-selective beam profiling arrays up to 1.2 THz are planned. The current detector chip readily detects THz fluences as low as 15 nJ cm^{-2} and hence does not require focusing of the THz beam. To ease the data acquisition, sequential readout of the detectors could be applied. However, this would lead to a loss of single-bunch information. Therefore a multi-channel analog pulse integration front-end is currently under development.

Acknowledgements

We thank the ELBE team for operating the TELBE facility.

Funding information

Funding for this research was provided by: Bundesministerium für Bildung und Forschung (InSEl grant No. 05K13ODB to ML, NN, DP, MG; SAMoS grant No. 05K16ODB to ML, NN, DP, MG); the European Cluster of Advanced Laser Light Sources (EUCALL) project which received funding from the European Union's Horizon 2020 research and innovation programme (grant No. 654220 to SK, BG, MG).

References

Abo-Bakr, M., Anders, W., Barday, R., Bondarenko, A., Bürkmann-Gehrlein, K., Dürr, V., Heßler, S., Jankowiak, A., Kamps, T., Knobloch, J., Kugler, O., Kuske, B., Kuske, P., Matveenko, A., Meseck, A., Müller, R., Neumann, A., Ott, K., Petenev, Y., Pflückhahn, D., Quast, T., Rahn, J. & Schubert, S. (2012). *BERLinPro Conceptual Design Report.* Helmholtz Zentrum Berlin, Germany.

Ackermann, W., Asova, G., Ayvazyan, V., Azima, A., Baboi, N., Bähr, J., Balandin, V., Beutner, B., Brandt, A., Bolzmann, A., Brinkmann, R., Brovko, O. I., Castellano, M., Castro, P., Catani, L., Chiadroni, E., Choroba, S., Cianchi, A., Costello, J. T., Cubaynes, D., Dardis, J., Decking, W., Delsim-Hashemi, H., Delserieys, A., Di Pirro, G., Dohlus, M., Düsterer, S., Eckhardt, A., Edwards, H. T., Faatz, B., Feldhaus, J., Flöttmann, K., Frisch, J., Fröhlich, L., Garvey, T., Gensch, U., Gerth, Ch., Görler, M., Golubeva, N., Grabosch, H.-J., Grecki, M., Grimm, O., Hacker, K., Hahn, U., Han, J. H., Honkavaara, K., Hott, T., Hüning, M., Ivanisenko, Y., Jaeschke, E., Jalmuzna, W., Jezynski, T., Kammering, R., Katalev, V., Kavanagh, K., Kennedy, E. T., Khodyachykh, S., Klose, K., Kocharyan, V., Körfer, M., Kollewe, M., Koprek, W., Korepanov, S., Kostin, D., Krassilnikov, M., Kube, G., Kuhlmann, M., Lewis, C. L. S., Lilje, L., Limberg, T., Lipka, D., Löhl, F., Luna, H., Luong, M., Martins, M., Meyer, M., Michelato, P., Miltchev, V., Möller, W. D., Monaco, L., Müller, W. F. O., Napieralski, O., Napoly, O., Nicolosi, P., Nölle, D., Nuñez, T., Oppelt, A., Pagani, C., Paparella, R., Pchalek, N., Pedregosa-Gutierrez, J., Petersen, B., Petrosyan, B., Petrosyan, G., Petrosyan, L., Pflüger, J., Plönjes, E., Poletto, L., Pozniak, K., Prat, E., Proch, D., Pucyk, P., Radcliffe, P., Redlin, H., Rehlich, K., Richter, M., Roehrs, M., Roensch, J., Romaniuk, R., Ross, M., Rossbach, J., Rybnikov, V., Sachwitz, M., Saldin, E. L., Sandner, W., Schlarb, H., Schmidt, B., Schmitz, M., Schmüser, P., Schneider, J. R., Schneidmiller, E. A., Schnepp, S., Schreiber, S.,

Seidel, M., Sertore, D., Shabunov, A. V., Simon, C., Simrock, S., Sombrowski, E., Sorokin, A. A., Spanknebel, P., Spesyvtsev, R., Staykov, L., Steffen, B., Stephan, F., Stulle, F., Thom, H., Tiedtke, K., Tischer, M., Toleikis, S., Treusch, R., Trines, D., Tsakov, I., Vogel, E., Weiland, T., Weise, H., Wellhöfer, M., Wendt, M., Will, I., Winter, A., Wittenburg, K., Wurth, W., Yeates, P., Yurkov, M. V., Zagorodnov, I. & Zapfe, K. (2007). *Nat. Photon.* **1**, 336–342.

Altarelli, M. (2011). *Nucl. Instrum. Methods Phys. Res. B*, **269**, 2845–2849.

Ball, P. (2017). *Nature (London)*, **548**, 507–508.

Brown, E. R. (2015). In *Semiconductor Terahertz Technology: Devices and Systems at Room Temperature Operation*, edited by G. Carpintero, L. E. G. Munoz, H. L. Hartnagel, S. Preu and A. V. Räisänen, ch. 5. Chichester: Wiley.

Casalbuoni, S., Schmidt, B., Schmüser, P., Arsov, V. & Wesch, S. (2009). *Phys. Rev. ST Accel. Beams*, **12**, 030705.

Cornell (2013). *Cornell Energy Recovery Linac*, https://www.classe.cornell.edu/Research/ERL/PDDR.html.

Dhillon, S. S., Vitiello, M. S., Linfield, E. H., Davies, A. G., Hoffmann, M. C., Booske, J., Paoloni, C., Gensch, M., Weightman, P., Williams, G. P., Castro-Camus, E., Cumming, D. R. S., Simoens, F., Escorcia-Carranza, I., Grant, J., Lucyszyn, S., Kuwata-Gonokami, M., Konishi, K., Koch, M., Schmuttenmaer, C. A., Cocker, T. L., Huber, R., Markelz, A. G., Taylor, Z. D., Wallace, V. P., Axel Zeitler, J., Sibik, J., Korter, T. M., Ellison, B., Rea, S., Goldsmith, P., Cooper, K. B., Appleby, R., Pardo, D., Huggard, P. G., Krozer, V., Shams, H., Fice, M., Renaud, C., Seeds, A., Stöhr, A., Naftaly, M., Ridler, N., Clarke, R., Cunningham, J. E. & Johnston, M. B. (2017). *J. Phys. D Appl. Phys.* **50**, 043001.

Dunning, M. P., Travish, G., Cohen, A., Frigola, P., Reiche, S. & Rosenzweig, J. (2007). *Int. J. Mod. Phys. A*, **22**, 4125–4133.

Emma, P., Akre, R., Arthur, J., Bionta, R., Bostedt, C., Bozek, J., Brachmann, A., Bucksbaum, P., Coffee, R., Decker, F.-J., Ding, Y., Dowell, D., Edstrom, S., Fisher, A., Frisch, J., Gilevich, S., Hastings, J., Hays, G., Hering, P., Huang, Z., Iverson, R., Loos, H., Messerschmidt, M., Miahnahri, A., Moeller, S., Nuhn, H.-D., Pile, G., Ratner, D., Rzepiela, J., Schultz, D., Smith, T., Stefan, P., Tompkins, H., Turner, J., Welch, J., White, W., Wu, J., Yocky, G. & Galayda, J. (2010). *Nat. Photon.* **4**, 641–647.

ESCC (2014). *1 μm Schottky diode process*, https://spacecomponents.org/epplcomponent/show?id=40025.

Gabriel, F., Gippner, P., Grosse, E., Janssen, D., Michel, P., Prade, H., Schamlott, A., Seidel, W., Wolf, A. & Wünsch, R. (2000). *Nucl. Instrum. Methods Phys. Res. B*, **161–163**, 1143–1147.

Galayda, J. (2014). *Proceedings of the 27th Linear Accelerator Conference (LINAC2014)*, 31 August–5 September 2014, Geneva, Switzerland. TUIOA04.

Green, B., Kovalev, S., Asgekar, V., Geloni, G., Lehnert, U., Golz, T., Kuntzsch, M., Bauer, C., Hauser, J., Voigtlaender, J., Wustmann, B., Koesterke, I., Schwarz, M., Freitag, M., Arnold, A., Teichert, J., Justus, M., Seidel, W., Ilgner, C., Awari, N., Nicoletti, D., Kaiser, S., Laplace, Y., Rajasekaran, S., Zhang, L., Winnerl, S., Schneider, H., Schay, G., Lorincz, I., Rauscher, A. A., Radu, I., Mährlein, S., Kim, T. H., Lee, J. S., Kampfrath, T., Wall, S., Heberle, J., Malnasi-Csizmadia, A., Steiger, A., Müller, A. S., Helm, M., Schramm, U., Cowan, T., Michel, P., Cavalleri, A., Fisher, A. S., Stojanovic, N. & Gensch, M. (2016). *Sci. Rep.* **6**, 22256.

Ho, L., Pepper, M. & Taday, P. (2008). *Nat. Photon.* **2**, 541.

Ishikawa, T., Aoyagi, H., Asaka, T., Asano, Y., Azumi, N., Bizen, T., Ego, H., Fukami, K., Fukui, T., Furukawa, Y., Goto, S., Hanaki, H., Hara, T., Hasegawa, T., Hatsui, T., Higashiya, A., Hirono, T., Hosoda, N., Ishii, M., Inagaki, T., Inubushi, Y., Itoga, T., Joti, Y., Kago, M., Kameshima, T., Kimura, H., Kirihara, Y., Kiyomichi, A., Kobayashi, T., Kondo, C., Kudo, T., Maesaka, H., Maréchal, X. M., Masuda, T., Matsubara, S., Matsumoto, T., Matsushita, T., Matsui, S., Nagasono, M., Nariyama, N., Ohashi, H., Ohata, T., Ohshima, T., Ono, S., Otake, Y., Saji, C., Sakurai, T., Sato, T., Sawada, K., Seike, T., Shirasawa, K., Sugimoto, T., Suzuki, S., Takahashi, S., Takebe, H., Takeshita, K., Tamasaku, K., Tanaka, H., Tanaka, R., Tanaka, T., Togashi, T., Togawa, K., Tokuhisa, A., Tomizawa, H., Tono, K., Wu, S., Yabashi, M., Yamaga, M., Yamashita, A., Yanagida, K., Zhang, C., Shintake, T., Kitamura, H. & Kumagai, N. (2012). *Nat. Photon.* **6**, 540–544.

Kang, H., Min, C., Heo, H., Kim, C., Yang, H., Kim, G., Nam, I., Baek, S. Y., Choi, H., Mun, G., Park, B. R., Suh, Y. J., Shin, D. C., Hu, J., Hong, J., Jung, S., Kim, S., Kim, K., Na, D., Park, S. S., Park, Y. J., Han, J., Jung, Y. G., Jeong, S. H., Lee, H. G., Lee, S., Lee, S., Lee, W., Oh, B., Suh, H. S., Parc, Y. W., Park, S., Kim, M. H., Jung, N., Kim, Y., Lee, M., Lee, B., Sung, C., Mok, I., Yang, J., Lee, C., Shin, H., Kim, J. H., Kim, Y., Lee, J. H., Park, S., Kim, J., Park, J., Eom, I., Rah, S., Kim, S., Nam, K. H., Park, J., Park, J., Kim, S., Kwon, S., Park, S. H., Kim, K. S., Hyun, H., Kim, S. N., Kim, S., Hwang, S., Kim, M. J., Lim, C., Yu, C., Kim, B., Kang, T., Kim, K., Kim, S., Lee, H., Lee, H., Park, K., Koo, T., Kim, D. & Ko, I. S. (2017). *Nat. Photon.* **11**, 708–713.

Kayali, S., Ponchak, G. & Shaw, R. (1996). *GaAs MMIC reliability assurance guideline for space applications.* JPL Publication 96-58. Jet Propulsion Laboratory, California Institute of Technology, Pasadena, CA, USA.

Keil, B. *et al.* (2010). *Proceedings of the First International Particle Accelerator Conference (IPAC2010)*, 23–28 May 2010, Kyoto, Japan. MOPE064.

Keil, B., Marinkovic, G., Stadler, M. & Lipka, D. (2014). *Proceedings of the 3rd International Beam Instrumentation Conference (IBIC'14)*, 14–18 September 2014, Monterey, CA, USA, pp. 665–669. WEPD11.

Kovalev, S., Green, B., Golz, T., Maehrlein, S., Stojanovic, N., Fisher, A. S., Kampfrath, T. & Gensch, M. (2017). *Struct. Dyn.* **4**, 024301.

Lai, R. & Sievers, A. J. (1997). *Nucl. Instrum. Methods Phys. Res. A*, **397**, 221–231.

Löhl, F., Arsov, V., Felber, M., Hacker, K., Jalmuzna, W., Lorbeer, B., Ludwig, F., Matthiesen, K.-H., Schlarb, H., Schmidt, B., Schmüser, P., Schulz, S., Szewinski, J., Winter, A. & Zemella, J. (2010). *Phys. Rev. Lett.* **104**, 144801.

Marchetti, B., Krasilnikov, M., Stephan, F. & Zagorodnov, I. (2014). *Phys. Procedia*, **52**, 80–89.

Maxwell, T. J., Behrens, C., Ding, Y., Fisher, A. S., Frisch, J., Huang, Z. & Loos, H. (2013). *Phys. Rev. Lett.* **111**, 184801.

Mehdi, I., Siles, J. V., Lee, C. & Schlecht, E. (2017). *Proc. IEEE*, **105**, 990–1007.

Murokh, A., Rosenzweig, J. B., Hogan, M., Suk, H., Travish, G. & Happek, U. (1998). *Nucl. Instrum. Methods Phys. Res. A*, **410**, 452–460.

Nodvick, J. S. & Saxon, D. S. (1954). *Phys. Rev.* **96**, 180–184.

Schiselski, M., Laabs, M., Neumann, N., Kovalev, S., Green, B., Gensch, M. & Plettemeier, D. (2016). *2016 IEEE MTT-S International Microwave Symposium (IMS)*, 22–27 May 2016, San Francisco, CA, USA, 2016, pp. 1–4.

Schmidt, B., Wesch, S., Kövener, T., Behrens, C., Hass, E., Casalbuoni, S. &Schmüser, P. (2018). *arXiv:*1803.00608.

Sokolnikov, A. U. (2013). *THz Identification for Defense and Security Purposes: Identifying Material, Substances and Items.* Singapore: World Scientific.

Waldrup, M. M. (2014). *Nature (London)*, **505**, 604.

Watanabe, T., Sugahara, J., Yoshimatsu, T., Sasaki, S., Sugiyama, Y., Ishi, K., Shibata, Y., Kondo, Y., Yoshii, K., Ueda, T. & Uesaka, M. (2002). *Nucl. Instrum. Methods Phys. Res. A*, **480**, 315–327.

Wesch, S., Schmidt, B., Behrens, C., Delsim-Hashemi, H. & Schmüser, P. (2011). *Nucl. Instrum. Methods Phys. Res. A*, **665**, 40–47.